

The effect of current density on the structures and photoluminescence of n-type porous silicon

Nada K. Abbas¹, Isam M. Ibrahim², Manal A. Saleh¹

¹Department of Physics, College of Science for Women, Baghdad University, Baghdad, Iraq

²Department of Physics, College of Science, Baghdad University, Baghdad, Iraq

E-mail: dr.issamiq@gmail.com

Abstract

Porous silicon (PS) layers were formed on n-type silicon (Si) wafers using Photo- electrochemical Etching technique (PEC) was used to produce porous silicon for n-type with orientation of (111). The effects of current density were investigated at: (10, 20, 30, 40, and 50) mA/cm² with etching time: 10min. X-ray diffraction studies showed distinct variations between the fresh silicon surface and the synthesized porous silicon. The maximum crystal size of Porous Silicon is (33.9nm) and minimum is (2.6nm) The Atomic force microscopy (AFM) analysis and Field Emission Scanning Electron Microscope (FESEM) were used to study the morphology of porous silicon layer. AFM results showed that root mean square (RMS) of roughness and the grain size of porous silicon decreased as etching current density increased and FESEM showed that a homogeneous pattern and confirms the formation of uniform porous silicon. The chemical bonding and structure were investigated by using Fourier transformation infrared spectroscopy (FTIR). The band gap of the samples obtained from photoluminescence (PL). These results showed that the band gap of porous silicon increase with increasing porosity.

Key words

Porous silicon, electrochemical etching, x-ray diffraction, morphological properties, FTIR spectra, photoluminescence.

Article info.

Received: Oct. 2016

Accepted: Jan. 2017

Published: Sep. 2017

تأثير كثافة التيار على الخصائص التركيبية وطيف اللمعان الضوئي للسيليكون المسامي من

النوع n

ندى خضير عباس¹، عصام محمد ابراهيم²، منال علي صالح¹

¹قسم الفيزياء، كلية العلوم للبنات، جامعة بغداد، بغداد، العراق

²قسم الفيزياء، كلية العلوم، جامعة بغداد، بغداد، العراق

الخلاصة

تم تشكيل طبقات السيليكون المسامي على شرائح السيليكون نوع n و ذو اتجاهية (111) باستخدام طريقة القشط الكهروكيميائي ودراسة تأثير اختلاف كثافة التيار (10, 20, 30, 40 and 50) mA على الخصائص التركيبية والبصريه للسيليكون المسامي وثبتت زمن القشط (10 ثواني). لقد اوضحت نتائج حيود الاشعة السينية XRD ان طيف التركيب المسامي يختلف عن نظيره البلوري حيث كان اعلى حجم بلوري 33.9 nm واقل حجم بلوري 2.6nm تم استخدام تقنية مجهر القوة الذرية AFM و دراسة طبوغرافية السطح باستخدام المجهر الماسح الألكتروني FESEM حيث اوضحت نتائج AFM ان مقدار الجذر التربيعي لمعدل خشونة السطح والحجم الحبيبي لسطح السيليكون المسامي قد يقل مع زيادة كثافة تيار التنميش. ان التركيب والتأصر الكيميائي للسيليكون المسامي تم فحصه بواسطة تقنية FTIR. اظهرت دراسة طيف اللمعان الضوئي للسيليكون المسامي بان فجوة الطاقة للسيليكون المسامي تزداد بزيادة المسامية.

Introduction

Porous silicon (PS) was discovered in 1956 by Ulhir [1] while performing electropolishing experiments on silicon wafers, using an electrolyte containing hydrofluoric acid (HF) under the appropriate applied current and solution composition, the spatial confinement of the excited carriers in small silicon regions. Porous Silicon (PS) is a nanostructured material based on silicon fabricate by electrochemical etching of crystalline silicon, which consists of assembly of holes (pores) and fibrils, rendering a large surface to volume ratio[2]. The silicon remained uniformly undissolved, but rather fine holes were produced [3]. PS formation was obtained by electrochemical dissolution of silicon wafers in aqueous or ethanoic HF solutions. In the 1970s and 1980s, interest in PS increased because its high surface area was found to be useful as a model of the crystalline silicon surface in spectroscopic studies [4], as a precursor to generate thick oxide layers on silicon and as a dielectric layer in capacitance based chemical sensors. In the 1990s Leigh Canham published his results on red luminescence [5] showed that certain PS materials can have large PL efficiency at room temperature in the visible a surprising result since the PL efficiency of bulk silicon is very low due to its indirect energy band gap and short non-radiative life time The reason of this is the partial dissolution of silicon, which causes, The formation of small silicon nanocrystals in the PS material, The reduction of the effective refractive index of PS with respect to silicon, and hence an increased light extraction efficiency from PS.

The quantum confinement phenomena lead to new properties, like photoluminescence or electroluminescence [6]. PS is classified according to the pore diameter, which can vary from a few nanometers to a few microns

depending on the formation parameters.

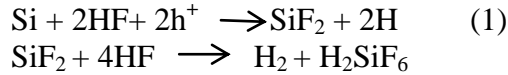
PS has been demonstrated to yield efficient visible light emission at room temperature due to its unique electrical, chemical, and mechanical properties as in comparison to bulk silicon, thus not quite suitable for the fabrication of optoelectronic devices[7, 8].

However, different hypothesis is reported on PL from PS surface. The first includes the quantum confinement effect which is due to the charge carriers in narrow crystalline silicon wall separating the pore walls. Later, many other alternative models were proposed based on hydrogenated amorphous silicon, surface hydrides, defects, siloxene, and surface states [9, 10]. Some properties of the PS layer, such as the refractive index, porosity, physical and optical thickness and pore diameter are strongly dependent on the etched parameters including HF concentration, current density, temperature and Si wafer type and resistivity [11, 12]. This paper investigated the effects of current density as variable factors simultaneously an attempt has been made to study the correlation between the, structural properties employing photoluminescence (PL) for porous silicon formed using n-type material under different conditions.

Experimental techniques

The schematic diagram of the experimental setup for preparing n-PS layer is given in Fig.1 the main body of the HF electrolyte container is made of Teflon materials. And, the apparatus is designed in a horizontal arrangement. Also, made of porous silicon produced with a standard technique of anodizing the PS samples are prepared on n- Si <111> substrates in an electrolyte a mixture of HF (40%): CH₃OH (99.8)% with a volume ratio of [1:1] is utilized

as the etching solvent in different volumes. The illustrative equation [1] of the overall process during PS formation can be expressed as below: Eq.(1).



In the equation, the etching rate is determined by the hole (h^+) generation. The anodization in galvanostatic (current-controlled) mode is used. It is normally preferred, because it supplies the required charge for the reaction at constant rate, regardless of any evolution during anodization of the cell electrical impedance, ultimately leading to more homogeneous and reproducible material. The anodization can be modulated. The modulation is most easily achieved by varying the applied current density [13, 14]. Modulation results in controlled changes of the microstructure and the porosity of PS along the growth direction.

The PS samples, investigated, were synthesized on n-type Si wafers by anodic etching using a conventional single-tank electrolyzation cell Fig.1. The wafers were polished along the (111) crystal plane direction. The electrolytes were prepared by mixing HF solution and absolute Methanol (CH_3OH) in various volumetric ratios.

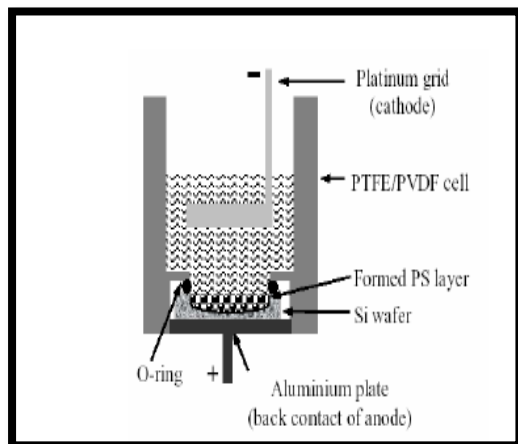


Fig.1: Schematic diagram of experimental set-up for preparing n-PS layer vertical arrangement.

The fabrication of Porous Silicon (PS) is a comparatively simple process that only requires a small amount of equipment, the simplest cell which can be used to anodize silicon. The silicon wafer serves as the anode. The cathode is made of platinum or any HF resistant and conducting material. The distance from the pole to the platinum Si is about 2 cm. The silicon wafers used were n-type, $\langle 111 \rangle$, double polished with a resistance of $10\Omega\cdot\text{cm}$. A self-made Teflon cell that etches a 1.5 cm^2 circular area on the wafer was used. The wafers were cut into pieces sufficient to contain this area by the scribe and cut method. The Si wafer first had to be diced $1.5 \times 1.5\text{ cm}^2$ (and smaller than for porosity) samples before cleaning. Cleaning is vital to remove particulate matter as well as any traces of organic, metallic and ionic contaminants from samples.

Aluminum foil covers the entire back side of the aluminum foil as the backside Contact. Together, sample and aluminum foil were sandwiched into the cell. The wafers were used as received; nothing was done to the either front or back-side. Surface of the wafer with Controllable parameters then become HF concentration, anodization time and light [15].

In the experiments, silicon wafers n-type, with samples are Methanol and alcohol are used commonly clean the wafer by immersing it in these chemicals In turn in the ultrasonic bath for few minutes. Finally, they were rinsed in distilled water treated ultrasonically followed by drying in a hot air stream. Porous silicon (PS) samples were prepared by anodization at a current density (10, 20, 30, 40, 50) mA/cm^2 at a constant times 10 min the manufacturing process shown in Fig.2.

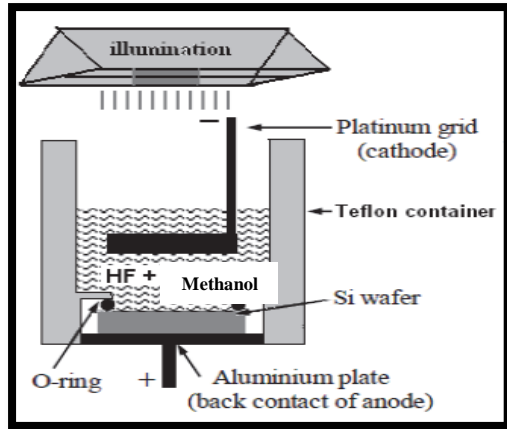


Fig.2: Schematic of the experimental setup of the illumination assisted method.

To get the nanocrystalline porous silicon on n-type silicon, illumination method just we need a photon source such as halogen lamp where the halogen power of 100 watts and the distance between the lamp and the Si (16) cm and intensive light is used to supply the required holes in the irradiated area of silicon wafer to initiate the etching process. The most popular way to generate holes required in the electrochemical etching process (Fig.2). However, the photo energy absorption by the atoms depends on the intensity of the illumination source, the distance from the source and the electrolyte environment. Therefore, only the surface layer under the illumination generates electron hole pairs. But the etching rate gradually decreases with time as it is very difficult to reach the illumination into the deep area of the pores.

The x-ray diffraction test is widely used as a characterization technique is recorded by "SHIMADZU" XRD-6000 X-ray diffract meter (CuK α radiation $\lambda=0.154$ nm) in the scanning angle 2θ varied of 10 – 80 degree with a speed of 4 deg/min.

The full width at half maximum (FWHM) of the peak in radians is a measure of the crystallite size samples, crystallite size, as described by Scherreris formula [16]:

$$C.S = 0.94\lambda / FWH \cdot \cos(\theta) \quad (2)$$

where: θ is the Bragg angle, λ :- Wavelength of the incident x-rays in angstroms 1.54 \AA , FWHM: full width at half maximum.

The morphological surface analysis was carried out by employing an atomic force microscope (AA3000 Scanning Probe Microscope SPM, tip NSC35/AIBS from Angstrom Advance Inc).

Field emission scanning electron microscopy (FE-SEM), equipped with Energy-Dispersive produce by Hitachi-Japan, model (S-4160FE-SEM) provides topographical and elemental information at magnifications of 10X to 300,000X, with virtually unlimited depth of field the samples with gold paint before an examination FESEM using a device Nano Structured Coating CO.DSR1.

Fourier Transform Infrared (FTIR) test is used to observe the spectra of PS samples utilizing a Bruker FTIR analyzer, Tensor-27, Bruker Optics Inc, Billerica, MA, using an attenuated total reflectance mode. The data were recorded in the range from 400 to 4000 cm^{-1} wave numbers.

The photoluminescence spectra of the PS, were measured using SL-174 (ELICO) Spectro Fluormeter, 150 watt Xenon Arc lamp, Excitation and emission from 300-700 nm using 250 nm as wavelength excitation. Photoluminescence is a non destructive and contactless method of probing the electron structure of materials. Photo-excitation occurs when light is directed onto a sample and it gets absorbed and imparts excess energy into the material. One of the ways, this excess energy can be dissipated by the sample through the emission of light this process is called (photoluminescence). The PS energy gap is definitely having higher energy gaps compare to silicon (1.11) eV and it increases from (2.4-

2.5) eV as etching time and porosity increased. The energy gap was determined by Eq.(3) [17]:

$$E_g = hc/\lambda \quad (3)$$

where: E_g is energy of PS. h is Planck constant, c the is speed of light, λ is the peak wavelength of the photoluminescence.

Results and discussion

XRD analyses show a typical diffraction pattern of PS sample fabricated at etching current density of (10, 20, 30, 40 and 50) mA/cm² respectively at etching time of 10 min formed during the Photo-electrochemical Etching technique (PEC) process. A structure of all the samples and most of them show.

Fig.3 shows the x-ray diffraction patterns of the porous structure on n-Si substrate at different current density respectively. X-ray diffraction spectra showed a distinct variation between the bulk silicon surface and the porous silicon surfaces formed at different anodizing current densities. The broadening in the diffracted peaks is due to the increasing of pore walls thickness, and upward shifts are due to relaxation of strain in the porous structure. The presences of their peaks of PS structures prove that the cubic structure of the crystalline silicon is retained even after the pore formation. The reduction in the crystallite size can be inferred through the increasing in the broadening of the x-ray diffraction spectra.

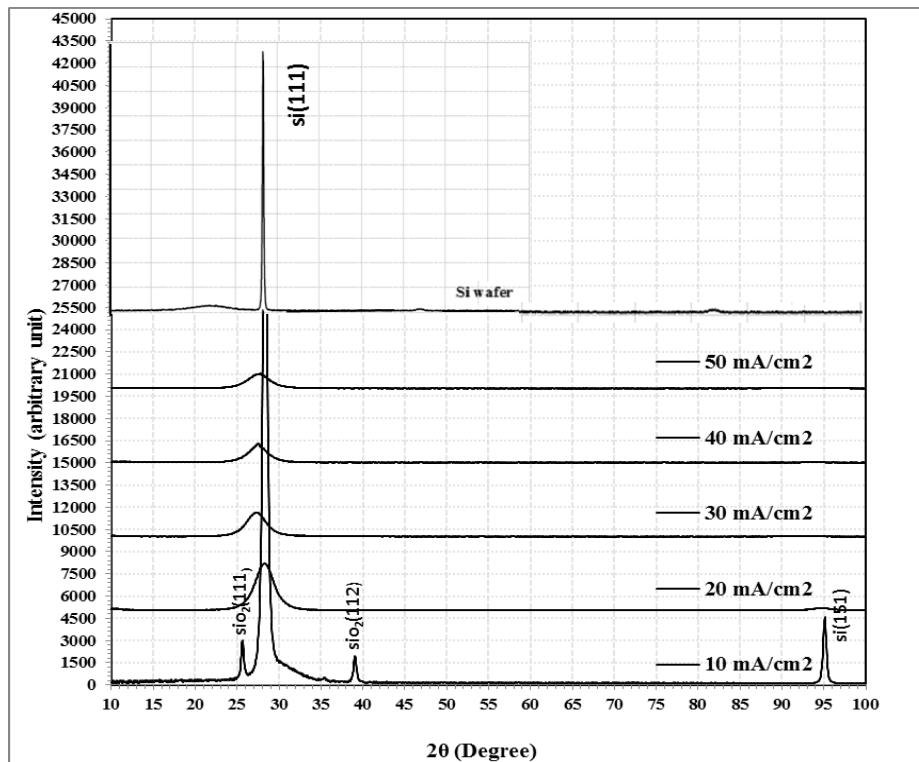


Fig. 3: X-ray diffraction patterns for PS with different etching current 10, 20, 30, 40 and 50 mA/cm².

The x-ray beam is diffracted at specific angular positions with respect to the incident beam depending on the phases of the sample. When crystal size is reduced toward nanometer scale, then a broadening of diffraction peaks

is observed and the width of the peak is directly correlated to the size of the nanocrystalline domains, which agrees with the results of (A. Lorusso et al. 2009, Luigi Russo et al., 2011) [18,19]. XRD spectra of bulk silicon showed a

very sharp peak at $2\theta = 28.3^\circ$ showing the single crystalline nature of the wafer. This peak becomes very broad with varying full width at half maximum (FWHM) for different anodization current densities as shown in Fig.3 which confirms the formation of pores on the crystalline silicon surface. When the current density is increased from 10 mA/cm^2 to 50 mA/cm^2 the number of pores increased with thicker silicon walls, where the

thickness of the porous structure is decreasing with increasing etching current; the reduction in the crystallite size as evident from the sharp nature of the (111) peak, which is in agreement with the results of (Uday M. Nayef et al., 2013) [20].

Table 1 shows the effect of an increasing of current density from (10, 20, 30, 40, and 50) mA/cm^2 this peak becomes broad with varying full-width at half maximum.

Table 1: Comparison between experimental d_{hkl} and standard d_{hkl} values of x-ray diffraction peaks for PS with different etching current 10, 20, 30, 40 and 50 mA.

sample	2θ (Deg.)	FWHM (Deg.)	Int. arb. Unit	d_{hkl} Exp.(Å)	G.S (nm)	d_{hkl} Std.(Å)	phase	hkl	Card No.
a	28.3100	0.2420	43000	3.1499	33.9	1.3620	Si	(111)	96-901-3108
	95.1020	0.2120	8600	1.0439	55.5	1.0485	Si	(151)	96-901-3108
b	25.6405	0.3760	2478	3.4715	21.7	3.4210	SiO ₂	(111)	96-900-8309
	28.3400	0.5880	41548	3.1467	13.9	1.3620	Si	(111)	96-901-3108
	39.0606	0.3970	1771	2.3042	21.2	2.2932	SiO ₂	(112)	96-900-8309
	95.1000	0.4350	4441	1.0440	27.1	1.0485	Si	(151)	96-901-3108
c	28.2600	2.6029	3170	3.1554	3.1	1.3620	Si	(111)	96-901-3108
	94.7500	2.8359	156	1.0469	4.1	1.0485	Si	(151)	96-901-3108
d	27.2800	2.7165	1619	3.2665	3.0	1.3620	Si	(111)	96-901-3108
e	27.4770	2.7607	1300	3.2435	3.0	1.3620	Si	(111)	96-901-3108
f	27.5500	3.0964	957	3.2351	2.6	1.3620	Si	(111)	96-901-3108

The structure of the surface morphology of the unsubstantiated, substantiate with PS layer fabricated. The surface morphology measured by AFM is given in Fig. 4 which shows the AFM images of porous silicon n-type at etching current density of (10, 20, 30, 40 and 50) mA/cm^2 and constant time of 10 min AFM measurements show that the surface of the etched PS layer consists of a matrix of randomly distributed nanocrystalline Si pillars and voids. When current flows in the electrochemical cell, the dissociation reaction localizes on a particular side of a silicon surface, thus starting the etching of an array of pores in the silicon wafer. The pore morphology was analyzed under conditions of varying current densities. At increasing in current density orders

the small pores to exhibit cylindrical shapes giving rise to larger pore diameter (Buda and Kohanoff, 1994; Beattie et al., 1995; Canham, 1997; Collins et al., 2002) [21]. For both cases irregular and randomly distributed nanocrystalline silicon and the voids over the entire surface that the dissociation reaction localized on the particular side of a silicon surface, thus initiating the etching of an array of pores in the silicon wafer increasing of the etching current density causes an increase in the pore size and decrease particle size. At high etching current density, a highly branchrandomly directed and highly inter-connected meshwork of pore was obtained which raiment with the results of (V.Parkhutik et al, 1999) [22].

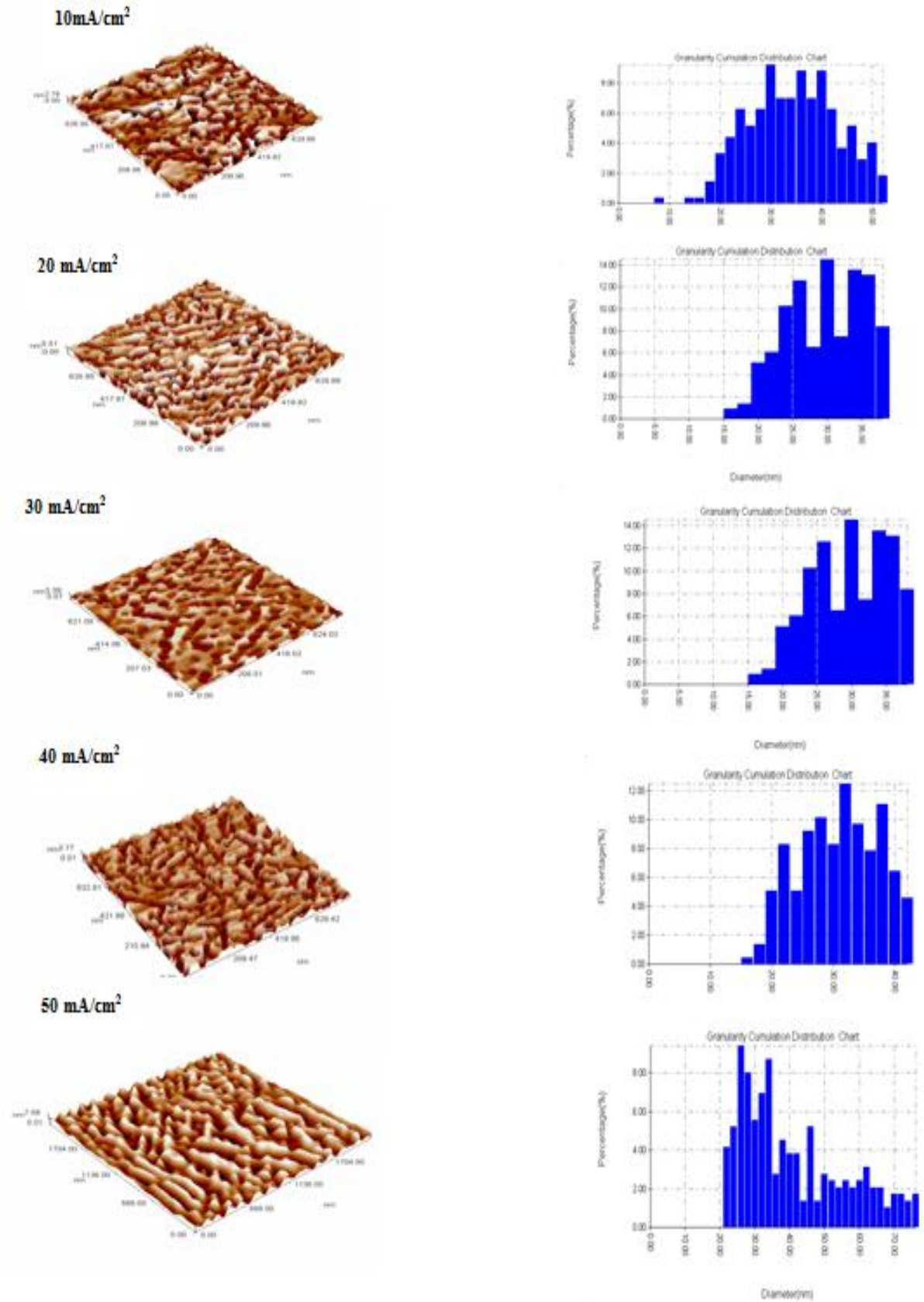


Fig. 4: 3D AFM images and size distribution for porous silicon at constant time and different etching current 10, 20, 30, 40 and 50 mA.

AFM parameters (average diameter, average roughness and peak –peak) for these samples have been shown in Table 2.

The average diameter decreased with increasing of the etching current density. A change of microstructure of the porous silicon surface were observed for different current densities where pores sizes varied significantly as shown in the AFM pictures. The surface of the etched PS layer consists of a matrix of randomly distributed nanocrystalline Si pillars which have the same direction and AFM

images also show voids that the uniformity. This roughness is expected to be caused by inhomogeneous of the substrate and electrolyte composition, this attributed to longer etching time caused an increasing in porosity, so the pores have begun again to grow and decreased in an average roughness. The uniform pore on the wafer was created, also the effect of H bubbles that were created at the surface of the sample lead to reduce of HF concentration, thus preventing further silicon dissolution [23].

Table 2: AFM parameters for porous silicon with constant time and different etching current 10, 20, 30, 40 and 50 mA.

Etching,current(mA/cm ²)	Avg.Diametr(nm)	Avg.Roughness(nm)	Peak-peak (nm)
10	40.12	1.64	7.08
20	33.48	0.687	2.79
30	29.79	0.81	3
40	28.56	1.42	5.5
50	28.00	0.597	2.47

Fig. 5 shows a typical FESEM image of PS(n-type) silicon the etched surface prepared under current density of (10, 20, 30, 40 and 50) mA/cm² and etching time of 10 min the porous layer composed of a dense large pore aligned in random direction. The effect of increasing current density 50mA on surface morphology is a group of PS is presented in structure pores in (FE-SEM) images and a homogeneous

pattern and confirms the formation of uniform porous structures on the silicon wafer. The increasing of current density causes an increase in the pore size [24].

The increase of current density means an increase of silicon dissolution process within the porous layer due to the increase of photo-generated holes number on the silicon electrode [25].

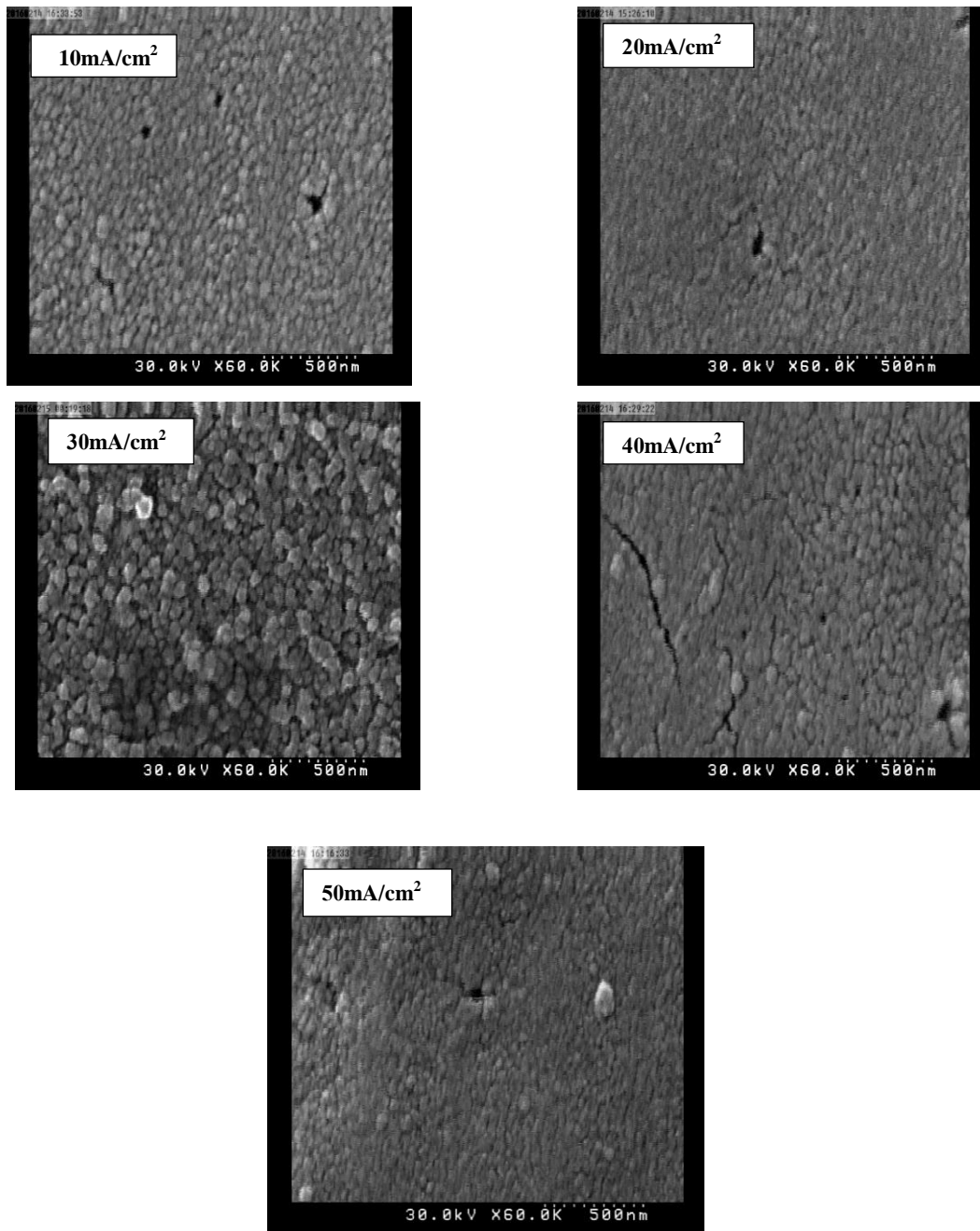


Fig. 5: FESEM image of n-type porous silicon surface with different current density 10, 20, 30, 40 and 50 mA.

Surface chemical composition of PS is best probed with Fourier transform infrared (FTIR) spectroscopy. FTIR signal in PS is larger and easier to measure than in bulk Si due to much larger specific area [26]. The pore surface includes a high density of dangling bonds of Si for original impurities such as hydrogen and fluorine, which are residuals from the electrolyte. Additionally, if the manufactured PS layer is stored in

ambient air for a few hours, the surface oxidizes spontaneously.

The Fourier transformation infrared spectroscopy FTIR of the measured for n-type PS at etching current densities values of (10, 20, 30, 40 and 50) mA/cm² with constant time 10 min. The different vibration modes are detected which described in Table 2. As can be seen from Fig. 6 after its anodization is completed, it is clear that there are five distinct peaks with

different intensities. A small peak at 625 to 2089/cm⁻¹ can be associated with the Si-H Waggener mode [27]. While a peak at 2926 to 2361/cm⁻¹ is suggests of the CH Asymmetric stretching [28]. The peak with intensity at 1071 to 1112/cm⁻¹ that indicates the presence of Si-O-Si Asymmetric stretching [29]. At etching current 50 mA/cm² peak at 1666/cm⁻¹ associated with the NH₂ Asymmetry stretch [30]. And finally at etching current (40 mA/cm²) the bond is related peak of 1724/cm⁻¹ CO bending [31].

The peak at about 625cm⁻¹ is attributed to the wagging modes of the SiH species. Absorption at 2926cm⁻¹ is due to the in plane C-H angle deformation It can easily replace a silicon atom, leading to the presence of carbon in the porous structure, since carbon is located in the same column of the periodic Table as silicon [32].

One may notice the presence of absorption bands associated to hydrolyze illustrated by different vibrational modes related to SiH₂ and CH₂ bonds. where one may point out stretching modes of CH₂ at 2326cm⁻¹, bands at 908-910 And 2104 cm⁻¹, These modes are related to groups SiH₂ adsorbed at the extended porous silicon surface, the initial spectrum remains almost identical, but the most relevant changes are produced near the frequencies related to silicon-oxygen bonds, the relevant vibration modes are centered at 1071 and 1080 cm⁻¹ A strong broad band is due to Si-O-Si asymmetry stretching absorption bands the relevant

vibrational modes are centered at 1071 and 1080 cm⁻¹, The signal at 1071 cm⁻¹ corresponds to the stretching modes of the Si-O-Si bridges in SiO₂ [33]. The peak at 1080 cm⁻¹ is generated by the asymmetrical stretching of Si-O-Si bridges in stoichiometric SiO₂. As this peak does not undergo important changes when the samples are processed, it can be argued that this mode is related to the silicon substrate. Otherwise, as the modes at 1071 and 1080 cm⁻¹ appear only in some oxidation degree, these frequencies can be related to the highly stressed SiO₂/Si interface or defective silicon oxide at the porous silicon surface. These modes are the symmetrical and antisymmetrical vibrational modes of the Si-O-Si bridges [34, 35].

The spectral region is characterized by two peak at 1666 related to the asymmetric and symmetric stretching modes of NH₂ respectively The 1666 cm⁻¹ related peakes are assigned to the NH₂ mation modes of the amine groups, which are very strongly hydrogen bonded the silanol groups.

Fig.7 presents photoluminescence (PL) spectra of the n-type porous silicon curves obtained in samples, prepared at different anodizing currents (10, 20, 30, 40 and 50mA) anodizing time: 10 minutes. It is clear from these figures that the emission signal shifts towards shorter wavelengths as the anodizing current porosity increases. Which is in agrees with the results of Bessais and O. Ben (Younes et al., 2000) [36].

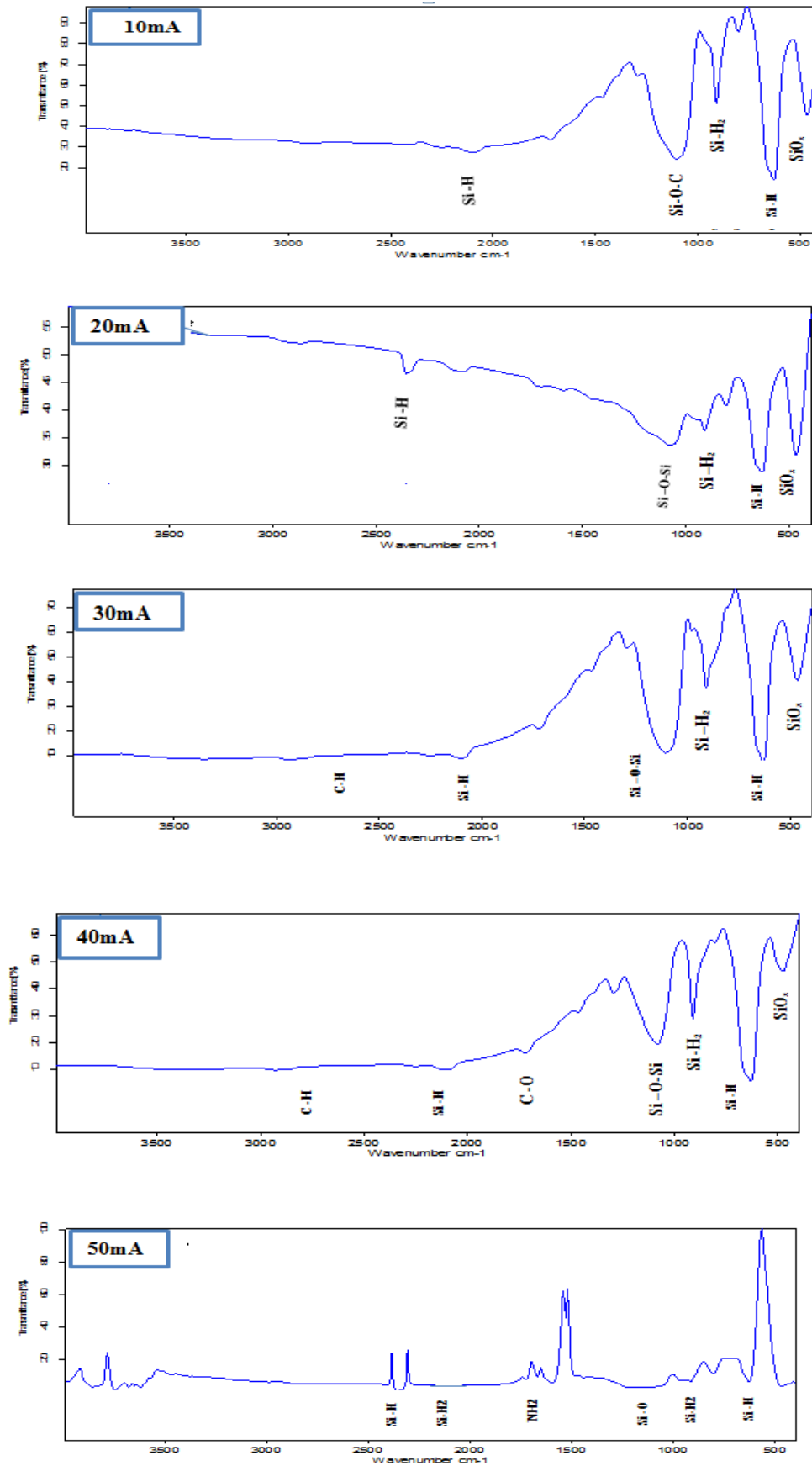


Fig. 6: IR transmittance spectrum of a PS layer at etching current density of 10, 20, 30, 40 and 50 mA.

Table 3: Wavenumber positions and attributions of the transmittance peaks observed in PS samples by FTIR measurements.

Functional group	Peak position (cm ⁻¹)	Peak Position ref (cm ⁻¹)	Bonds	Attribution
Si-H	625.77	626	Si-H	Wagging mode
	628.35		Si-H	Wagging mode
	630.94		Si-H	Wagging mode
	2089.70	2088	Si-H	Stretching
	907.81		Si-H ₂	Scissors
	908.85		Si-H ₂	Scissors
	910.00		Si-H ₂	Scissors
	913.29		Si-H ₂	Stretching
2104.67	2106	Si-H ₂	Scissors	
Si-O-Si	466.65	466	Si-O	Stretching in O-Si-O
	1071.37	1072	Si-O-Si	Asymmetry stretch
	1080.61	1080	Si-O-Si	Asymmetry stretch
	1104.03	1104	Si-O-C	Stretching in O-Si-O
	1112.26	1112	Si-O	Asymmetry stretch
C-H	2926.70	2915-2930	C-H	Asymmetric stretching symmetric stretching
	2361.59		2326	
NH ₂	1666.48	1600	NH ₂	Asymmetry stretch
C-O	1724	1720-1750	C-O	Bending

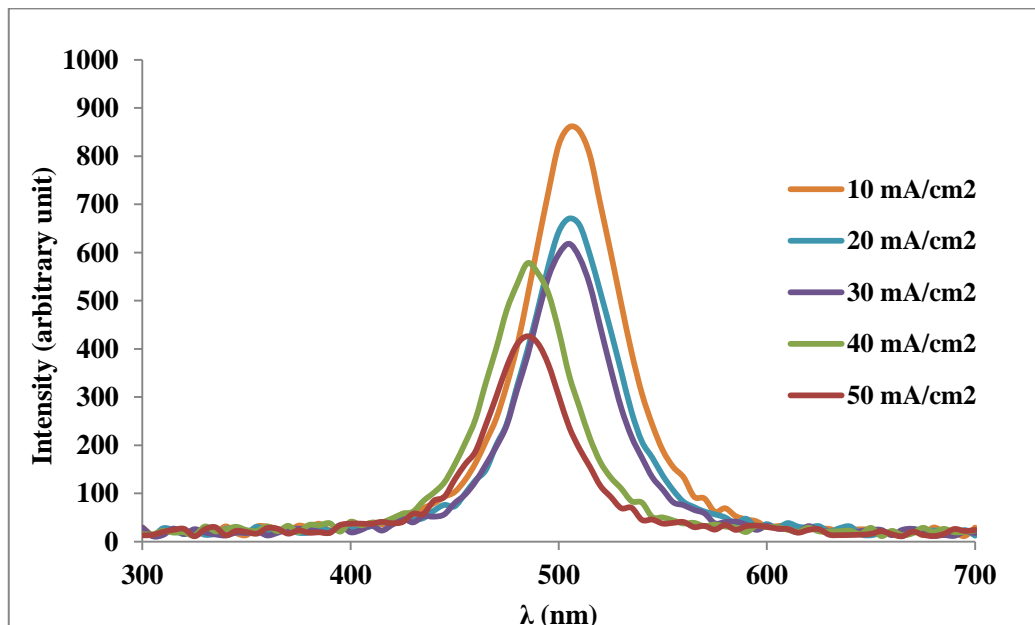


Fig. 7: The photoluminescence spectrum of PS which prepared at different etching current 10, 20, 30, 40, 50mA.

The band gap is calculated for each sample from the PL emission and the band gaps are given in Table 4. For all

samples, the band gap increased (band gap widening) is due to reduction in the particle size of the Si

nanocrystallite, porosity increases largely with increase in etching current density (10 - 50 mA/cm²) and constant etching time 10 min, due to change in the Si structure size [37]. The particle size of PS (111) grown in PS samples are low this is also reason for the shift in band gap blue shift is expected because of decrease in particle size of n-PS and increase in porosity and the

current density increases so the band gap increases, which is in agrees with the results of (Qing Shen et al., 2003)[38].

At the same time, the porosity of etching samples is confined to low current densities this result agreement with the XRD diffraction, AFM and FESEM.

Table 4: PL parameters for PS wafer with different etching current 10, 20, 40, 50 mA.

current density(mA/cm ²)	Wave length(nm)	Energy gap(eV)
10	507	2.446
20	506	2.451
30	504	2.460
40	486	2.551
50	485	2.557

IV Conclusions

1. n-type porous silicon synthesized by electrochemical etching at different current densities at etching time 10 min are found strongly dependence on etching current.
2. XRD spectra show that PS (n type) peak become broad when compressed with c-Si due to shifting of diffraction angle in nanowalls between pores of PS layers.
3. The AFM image shows that PS (n-type) has sponge like structure.
4. The Field emission scanning electron microscope (FESEM) indicates to the existence of smooth grain morphology of the film and the film preferentially grows parallel to the surface The increasing of current density causes an increase in the pore size
5. The FTIR Spectral show that PS Surface consist from active group from Si-Si bonds, Si-H bonds, Si-O and carbon component this come from interaction between c-Si and HF solution and interaction of PS with atmosphere.
6. PL spectral of PS was shifting to blue region due to quantum confinement effects from PL peak we

found increasing in energy gap of PS because the grain size is decrease.

References

- [1] Asra Behzad, Wan Mahmood Mat Yunus, Zainal Abidin Talib, Azmi Zakaria, Afarin Bahrami, Int. J. Electrochem. Sci., 7 (2012) 8266-8275.
- [2] Adina Bragaru, Monica Simion, Mihaela Miu, Teodora Ignat, Irina Kleps, Veronica SchIopu, Andrei Avram, Florin Cr̃Aciunoiu, 11, 4, (2008) 397-407.
- [3] A. Ulhir, AT &T. Tech. J., 2, 1-2 (1994) 101-112.
- [4] C.C. Striemer and P.M. Fauchet, Appl. Phys. Lett., 81 (2002) 2980-2982.
- [5] L.T. Canham, Adv. Mater, 7, 12 (1995) 1033-1037.
- [6] A. J. Cullis, L. T. Canham, P. D. J. Calcott, J. Appl. Phy., 82 (1997) 909-965.
- [7] Z. Gaburro, N. DaledOsso, L. Paves, Trento University Italy, 2004.
- [8] S. Adachi and Tomoo Kubota, J. of Porous Mater, 15 (2008) 427-431.

- [9] A. Ramizy, Z. Hassan, Khalid Omar, Science China, Technological Sciences, 54, 1 (2011) 58-62.
- [10] R. S. Dubey and D. K. Gautam, J. of Optoelectronic and Biomedical Materials, 1, 1 (2009) 8-14.
- [11] M. Jayachandran, M. Paramasivam, K.R. Murali, D.C. Trivedi, M. Raghavan, Mater Phys. Mech., 4 (2001) 143-147.
- [12] L. Yongfu, J. of Semiconductors, 32, 4 (2011) 1-4.
- [13] Jia-Chuan Lin, Wei-Lun Chen, Wei-Chih Tsai, "Optics Express", 14, 21 (2006) 47-52.
- [14] Yue Zhao, Deren Yang, Dongsheng Li, Minghua Jiang, Applied Surface Science, 252 (2005) 1065-1069.
- [15] Lu, G. Q. and X. S. Zhao. Nanoporous Materials, College Press Vol. 4, 2004.
- [16] K. Matsukawa, K. Shirai, H. Yamaguchi, H. Katayama-Yoshida, Phys. B Phys. Condens. Matter, (2007) 401-402, 151-154.
- [17] L. L. Yang, "Synthesis and Optical Properties of ZnO Nanostructures", Physical Electronic Division, Department of Science and Technology, Licentiate Thesis No.1384, Linköping University, Sweden (2008).
- [18] Dwight Tham Jern Ee, Chan Kok Sheng, M.I.N. Isa, The Malaysian Journal of Analytical Sciences, 15, 2 (2011) 227-231.
- [19] Lorusso, A. V. Nassisi, G. Congedo, N. Lovergine, L. Velardi, P. Prete, Applied Surface Science, 255 (2009) 5401-5404.
- [20] Uday M. Nayef and Ayoub H. Jaafar, Eng. & Tech. Journal, 31, 3 (2013) 341-342.
- [21] A.K. Patel, J. of Appl. Sci. Engineering and Technology, 2, 3 (2010) 208-215.
- [22] V. Parkhutik, Solid-state Electron, 43 (1999) 1121-1141.
- [23] W. O. Gordon, Virginia Polytechnic Institute and State University, Blacksburg, 2006.
- [24] M.V. Chursanova, L.P. Germash, V.O. Yukhymchuk, V.M. Dzhagan, I.A. Khodasevich, D. Cojoc, Appl. Sur. Sci., 256 (2010) 3369-3373.
- [25] S. L. Zhang, F. M. Huang, K. S. Ho, L. Jia, C. L. Yang, J.J. Li, T. Zhu, Y. Chen, S. M. Cai, A. Fujishima, Z. F. Liu, Phys. Rev., 58 (1998) 7-15.
- [26] W.J. Salcedo, F.J. R. Fernandez, E. Galeazzo, Brazilian Journal of Physics, 27, 4 (1997) 158-161.
- [27] A. Yu. Panarin, S.N. Terekhov, K.I. Kholostov, V.P. Bondarenko, 256 (2010) 6969-6976.
- [28] W.J. Salcedo, F.J. R. Fernandez, E. Galeazzo, Brazilian Journal of Physics, 27, 4 (1997) 158-161.
- [29] M.A.Vasquez, G.A.Rodreguez, G.G.Salgado, G.R.Paredes, R.P. Sierra, Revista Mexicana de Fisica, 53, 6 (2007) 431-435.
- [30] R. Pena- Alonso, F. Rubio. J. Rubio. J.I. Oteo, J. mater. Sci., 42 (2007) 595-603.
- [31] F. Razi, F. Rahimi, A. Irajizad, Sensors and Actuators B, ELSEVIER, vol 132, 2008.
- [32] J.P. Kar, S. K.Mothanta, G. Bose, S.Tuli, A.Kamra, V. Mathur, Journal of Optoelectronic and Advanced Material, 11, 3 (2009) 238-242.
- [33] R.R. Koropeccki and R. Arce, J. Appl. Phys., 60 (1986) 1802.
- [34] F. Ch'avez Ram'irez, Tesis de Doctorado, Ing. El'ectrica, CINVESTAV-IPN, 2003.
- [35] H. Yorikawa and S. Muramatsu, J. Luminescence, 87 (2000) 423-425.
- [36] O. Bisi, S. Ossicini, L. Pavesi, Surf Sci. Rep., 38 (2000) 1-126.
- [37] R. Cardenas, J. Torres, J. E. Alfonso, Thin Solid Films, 1-2, 478 (2005) 146-151.
- [38] Qing Shen and Taro Toyoda, Rev. Sci. Instr., 74, 601 (2003).